ACS APPLIED MATERIALS & INTERFACES

RESEARCH ARTICLE

www.acsami.org

Influences of pH and Ligand Type on the Performance of Inorganic Aqueous Precursor-Derived ZnO Thin Film Transistors

Taehwan Jun, Yangho Jung, Keunkyu Song, and Jooho Moon*

Department of Materials Science and Engineering, Yonsei University, 50 Yonsei-ro Seodaemun-gu, Seoul 120-749, Korea

S Supporting Information

ABSTRACT: The aqueous precursor-derived ZnO semiconductor is a promising alternative to organic semiconductors and amorphous silicon materials in applications requiring transparent thin-film transistors at low temperatures. The pH in the aqueous solution is an important factor in determining the device performance of ZnO-TFTs. Using a basic aqueous solution, the ZnO transistor annealed at 150 °C exhibited a high field-effect mobility (0.42 $cm^2\ V^{-1}\ s^{-1}$) and an excellent on/off ratio (10^6). In contrast, the ZnO layer annealed at 150 °C prepared from an acidic solution was inactive. Chemical and structural analyses confirmed that the variation of the device characteristics originates from the existing state difference of Zn in solution. The hydroxyo ligand is stable in basic conditions, which involves a lower energy pathway for the solution-to-solid conversion, whereas the hydrated zinc cation undergoes more complex reactions that occur at a higher temperature. Our results suggest that the pH and ligand type play critical roles in the preparation of aqueous precursor-based ZnO-TFTs which demonstrate high performance at low temperatures.

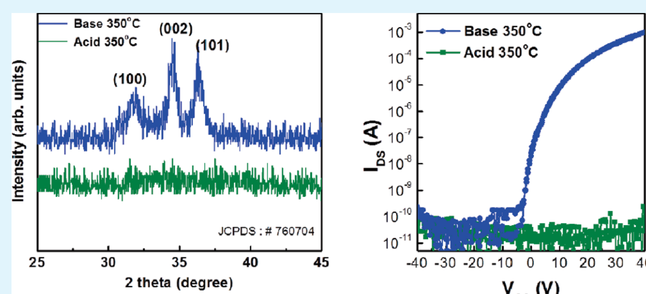

KEYWORDS: oxide semiconductor, thin film transistors, solution processing, aqueous solution, pH

INTRODUCTION

Oxide thin film transistors (TFTs) have attracted considerable attention because of their superior material properties, including their band gap, transparency, and high field effect mobility compared to conventional a-Si:H and organic semicondoctors in applications requiring tansparent TFTs. These materials meet the combined requirements of high-performance semiconducting active layers and low-temperature processing capabilities for the development of flexible electronics.[1−4] Oxide semiconductor thin films have been deposited primarily using vacuum-based physical vapor deposition techniques. TFTs based on an oxide semiconductor exhibit electron mobilities >10 $cm^2\ V^{-1}\ s^{-1}$, even for the channel grown near room temperature.[5,6] While these oxide semiconductors are considered emerging materials for transparent TFTs and unconventional electronics applications, vacuum processing significantly increases the manufacturing costs and poses major obstacles for realizing modern large-area, inexpensive electronics. In contrast, solution-processed TFTs can offer low-cost thin film transistor array/circuits via roll-to-roll processes using a combination of spin coating and printing techniques.[7−9]

Recently, several groups have explored solution techniques for depositing TFT-quality oxide semiconductors. However, conventional sol−gel processing with metal organic compounds requires large quantities of stabilizing reagents and organic solvents in the precursor solution.[10,11] High performance channel layers produced by a metal organic compound were obtained only when annealed at temperatures typically above 350 °C. With an annealing temperature under 350 °C, oxide TFTs did not show reasonable device properties.[9,12] Because high annealing temperatures (350 °C or more) are required to decompose the organic additives as well as facilitate the crystallization of the semiconducting oxides, sol−gel-derived materials are incompatible with low-cost and flexible plastic substrates.

In contrast, Meyers et al. employed an aqueous Zn precursor based on a metal ammine complex in an ammonium hydroxide solution, which resulted in low-temperature conversion into crystalline ZnO.[13] This approach relies on accelerating M−OH interactions within the aqueous precursor solution, reducing the need to use a high volume of organic ligands, leading to smooth and dense films through dehydration and condensation reactions.[14] In a similar approach, Fleischhakers et al. demonstrated a ZnO field-effect transistor on PEN foil using ZnO powder and aqueous ammonia.[15] We also synthesized an aqueous inorganic precursor by direct dissolution of zinc hydroxide in an ammonium hydroxide solution. With the combined use of microwave annealing, solution-processed ZnO-TFTs at 140 °C showed a device mobility of ∼1.7 $cm^2\ V^{-1}\ s^{-1}$.[16] It should be noted that all of the above-mentioned previous works focused on the solution-derived ZnO under basic conditions. It is considered that the aqueous zinc precursor under basic conditions results in better device performance as compared to acidic conditions. However, no detailed investigation was performed to understand why the pH of the aqueous precursor solution influences the ZnO-TFTs.

Received: November 17, 2010
Accepted: February 15, 2011
Published: March 02, 2011

 © 2011 American Chemical Society

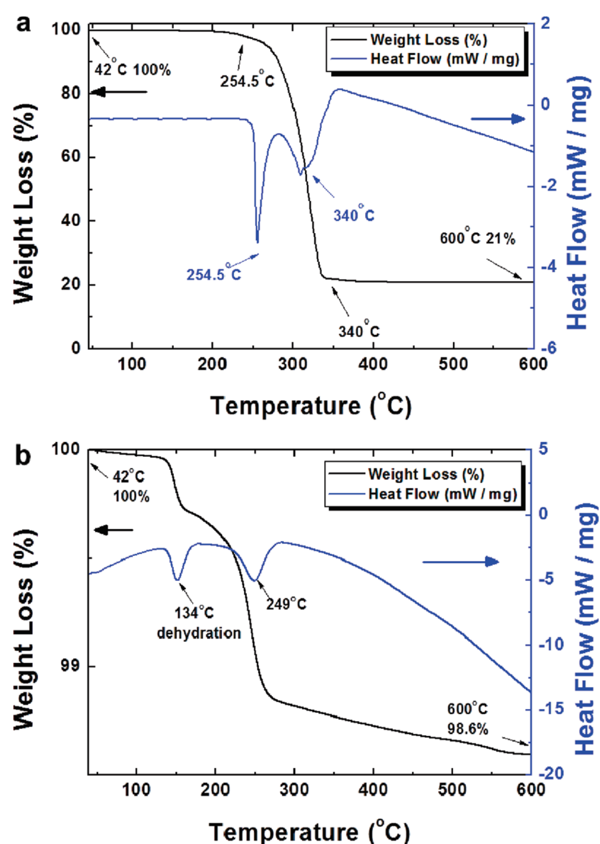

Figure 1. Thermogravimetric analysis and differential scanning calorimeter curves of the aqueous Zn precursor-based as-dried powders prepared under (a) acidic and (b) basic conditions.

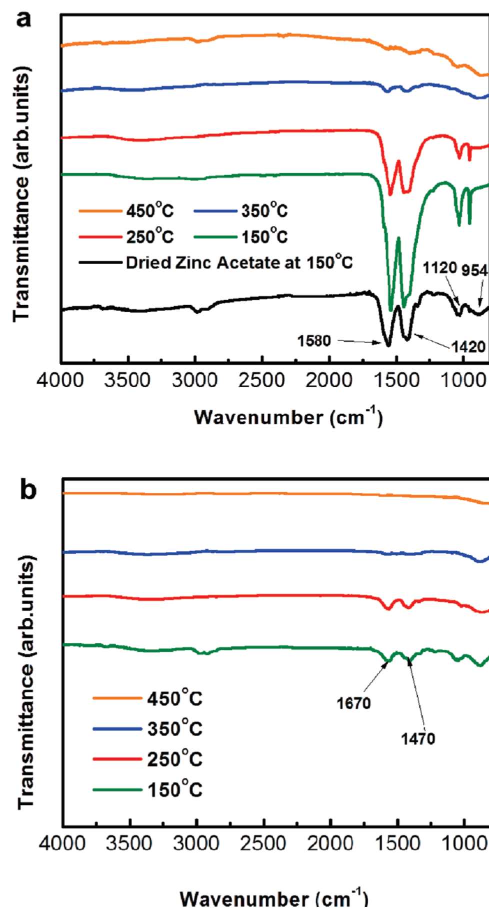

Figure 2. Fourier transform infrared (FTIR) spectra of the aqueous Zn precursor-derived films as functions of the annealing temperature and pH: (a) acidic and (b) basic conditions. The spectrum of zinc acetate dried at 150 °C is also shown in part a.

The pH is an important factor in determining the existing state of the soluble zinc species in the aqueous solution.[17,18] In aqueous solutions at high pH, the soluble species forms metal hydroxo ligands (M−OH), which require only a simple dehydroxylation/dehydration reaction to be converted to metal oxide (M−O). In contrast, at low pH, the stable species is a hydrated metal cation such as $M(H_2O)^{z+}$, where z is the valence number of the metal.[19,20] The as-spin-coated films produced under acidic conditions will undergo more complex reactions compared to those under basic conditions, such as anion decomposition during annealing. Much of the research in this field also proposed that basic conditions are essential for the formation of ZnO in aqueous solution systems. It has been reported that the pH determines the extent of hydrolysis of Zn ions in aqueous solution systems and is key to forming ZnO particles with controlled one-dimensional shapes.[21−23] In this paper, we focused on the influence of pH and ligand type on the performance of aqeuous precursor-based ZnO-TFTs. The device characteristics of the solution processed transistors as a function of pH and ligand type were investigated in conjuction with the structural and chemical analyses. Our results indicate that there is a suitable pH to form the soluble Zn species with a desirable ligand from which high-performance ZnO-TFTs are obtained at low temperatures.

RESULTS AND DISCUSSION

The starting Zn solutions were prepared by directly dissolving $Zn(OH)_2$ in either aqueous acetic acid (low pH) or ammonia solutions (high pH; for more details, see the Methods section). Figure 1 shows the thermal behavior of the precursor obtained by drying the aqueous Zn solution prepared under different pH conditions. Thermogravimetry differential scanning calorimetry (TG-DSC) of the as-dried precursor prepared at 120 °C from the acetic acid based solution was monitored under an amibient atmosphere, as shown in Figure 1a. The weight loss at ∼250 °C accounts for evaporation of the residual solvent. The significant weight loss and endothermic reaction at 340 °C indicates the vaporization/decomposition of the organic component.[24] No significant weight loss or noticeable heat transfer occurred at temperatures above 350 °C. Figure 1b shows the thermal behavior of the as-dried precursor produced at 120 °C from the ammonium hydroxide based solution. Although the precursor solutions were dried at the same temperature, the total weight loss when heated up to 600 °C was only 1.4%, as compared to 79% for the sample prepared under acidic conditions. This indicates a significant volume difference of volatile species including organic components in the as-dried precursors. The endothermic peak accompanying the weight loss at 134 °C can be attributed to the evaporation of water and ammonia, as well as dehydration, since crystalline ZnO is reported to form at a low temperature (above 134 °C).[25] An additional endothermic peak was observed at 249 °C.

A Fourier transform infrared spectrometer (FT-IR) was utilized to confirm the chemical composition of the films prepared under different pH conditions. Figure 2a shows the IR spectra of the as-dried films prepared at 150 °C for 2 h by spin-coating the acidic aqueous Zn solution as a function of the annealing temperature. The peaks at around 1580 and 1420 cm^{-1} are thought to be the

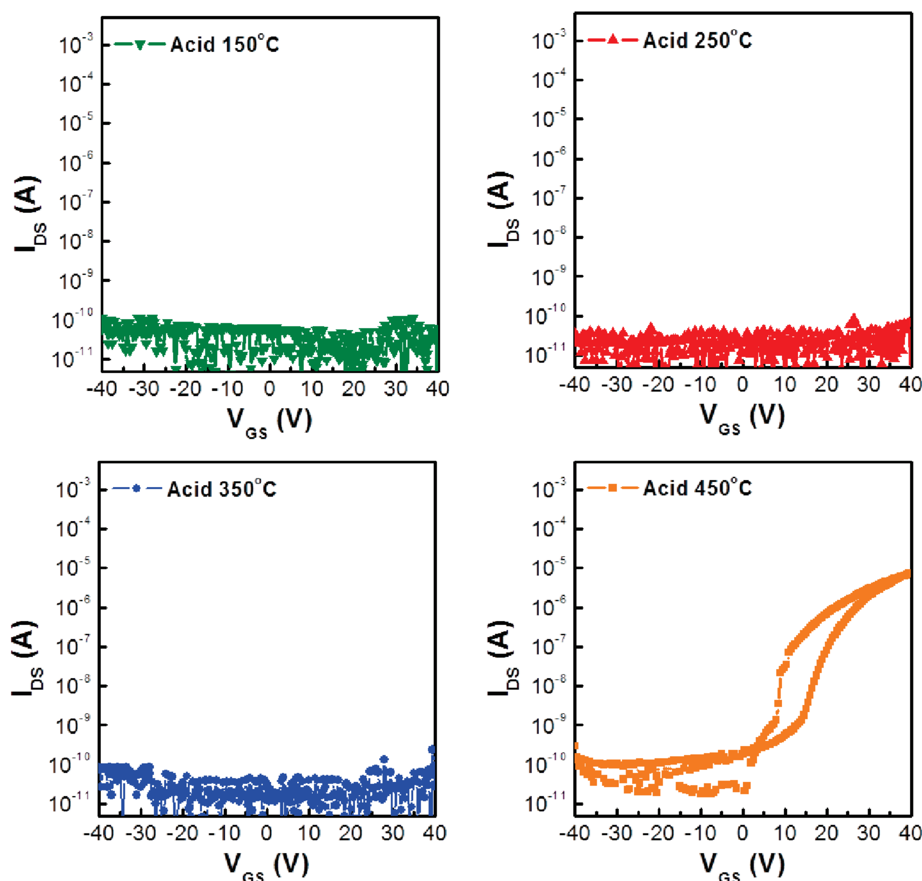

Figure 3. Transfer characteristics of the aqueous precursor-derived ZnO-TFTs prepared under acidic conditions on SiO_2/n^+-Si substrates as a function of the annealing temperature.

antisymmetric and symmetric stretchings of the carboxylate of zinc acetate, respectively.[26] The stretching modes of the C−O and C−C bond vibrations in the carboxylate group give rise to absorptions in the 1120−954 cm^{-1} region. The as-dried zinc acetate dihydrate powder annealed at 150 °C shows similar peak positions to those of the as-dried precursor film annealed at 150 °C prepared under acid conditions, as shown in Figure 2a. This observation confirms that the as-dried film is composed of zinc acetate. The peaks near 1580 and 1420 cm^{-1} were still obvious until the as-dried film was heated to 350 °C. Contrary to the TG-DSC results, the carboxylate group combined with Zn^{2+} species in the acetic acid solution exists in a stable state up to a temperature of 350 °C. With increasing heating temperature, the intensities of the peaks at around 1580 and 1420 cm^{-1} as well as the peaks near 1120 and 954 cm^{-1} gradually decreased. These peaks then disappeared when the as-dried films were heated to 450 °C. These results indicate that the organic components require high-temperature annealing to be decomposed. The FT-IR analysis indicates that the semiconducting characteristics of the channel made under acidic conditions are discernible after annealing at temperatures over 350 °C. Below this temperature, organic residues can act as obstacles for charge carrier accumulation and transportation in the conduction band.

Figure 2b shows the FT-IR spectra of the as-dried films produced by spin-coating the basic aqueous Zn solution as a function of the annealing temperature. The as-dried film annealed at 150 °C shows weak peaks at 1470 and 1613 cm^{-1}, which possibly correspond to the asymmetric and symmetric stretching vibrations of N−H bonds, respectively.[27] These peaks with reduced intensities exist in a stable state until 250 °C and then disappear at 350 °C. The endothermic peak observed at 249 °C in Figure 1b likely represents the decomposition of the Zn−ammine complex. Meyers et al. reported that Zn^{2+} soluble species form complexes such as $Zn(OH)_x(NH_3)_y^{(2-x)+}$ in ammonia−water solutions, followed by dehydration and crystallization at a low temperature (∼134 °C). In other words, the hydroxyl and ammine ligands in the Zn complex are labile bondings which easily volatilize at a low temperature.[13]

The TG-DSC and FT-IR results clearly show that the pH of the aqueous precursor determines the state of the soluble species of Zn. The pH of the precursor solution dissolved in acetic acid was 4.7, at which the Zn^{2+} is predominant over $ZnOH^+$ with a fraction of 0.9999 among the total dissolved Zn species, as calculated from the solubility diagram of $Zn(OH)_2$.[21] The Zn^{2+} cations become octahedrally coordinated to form the hexaqua ion, $Zn(OH_2)_6^{2+}$. Under these pH conditions, the acetic acid partially dissociates, releasing the acetic anion. Anion (X^-) complexation may also occur to form $ZnX(OH_2)_5^+$ in solution, depending upon the type of anion. The Zn acetate hydrate ($ZnX_2 \cdot xH_2O$) forms during the spin-coating as the water evaporates. After dehydration, the Zn acetate decomposes gradually to form ZnO according to the following reactions:[28]

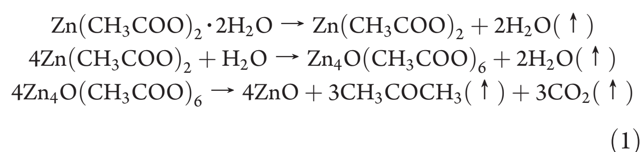

$$\begin{aligned} &Zn(CH_3COO)_2 \cdot 2H_2O \rightarrow Zn(CH_3COO)_2 + 2H_2O(\uparrow) \\ &4Zn(CH_3COO)_2 + H_2O \rightarrow Zn_4O(CH_3COO)_6 + 2H_2O(\uparrow) \\ &4Zn_4O(CH_3COO)_6 \rightarrow 4ZnO + 3CH_3COCH_3(\uparrow) + 3CO_2(\uparrow) \end{aligned} \quad (1)$$

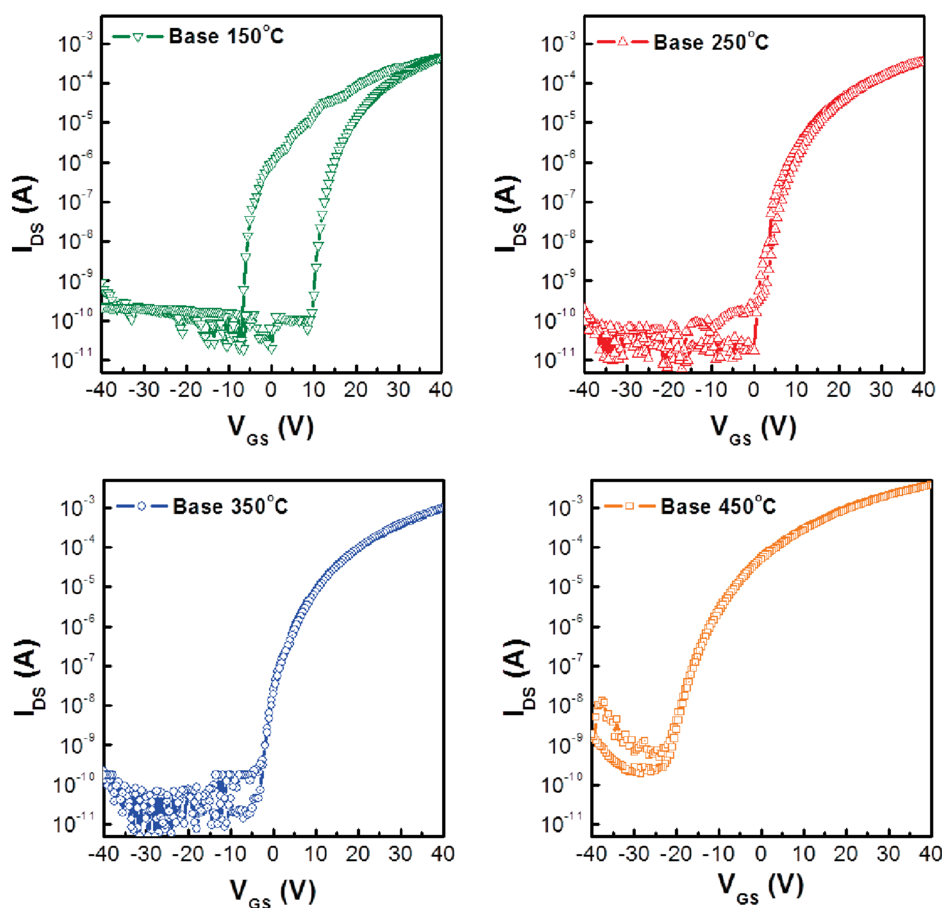

Figure 4. Transfer characteristics of the aqueous precursor-derived ZnO-TFTs prepared under basic conditions on SiO_2/n^+-Si substrates as a function of the annealing temperature.

The decomposition and dehydroxylation/dehydration reactions involve complex intermediate states and multiple steps with a high energy barrier for the conversion to metal oxide, requiring high temperature annealing above ~350 °C. The elimination of these complexes is a prerequisite for the conversion to ZnO and its crystallization. The precursor powders were similarly obtained by drying the aqueous Zn solution prepared by the dissolution of zinc hydroxide in nitric acid at 120 °C. The reactions come to completion at a similar temperature of 350 °C (see Supporting Information, Figure S1). These as-dried powders mainly consist of zinc nitrate. In the case of zinc chloride that forms upon the drying of the Zn precusor obtained by dissolution of $Zn(OH)_2$ in HCl, it was also reported that its decomposition and dehydroxylation/dehydration reactions occur at about 380 °C.[29] Although the decomposition temperatures are different depending upon the anion type, these observations indicate that the aqueous precursors prepared at low pH require high annealing temperatures to form the metal oxide regardless of the type of acids. That is, the dissolution of $Zn(OH)_2$ results in $Zn(OH_2)_6^{2+}$ soluble species under low pH conditions from which the zinc salts form during drying by strong electrostatic attractions with soluble anionic species since the hydroxo ligand is not available in the low pH range. The resulting zinc salts need the high annealing temperature to transform into ZnO. Under basic conditions, on the other hand, the soluble hexaaqua zinc species becomes destabilized with increasing pH due to its tendency to deprotonate and undergo hydrolysis. Zinc-coordinated water molecules are deprotonated, leading to the formation of a metal hydroxo ligand such as $Zn(OH)_4^{2-}$.[30] Ammonia also complexes with Zn to form aqueous ammine−hydroxo zinc complexes such as $Zn(OH)_x(NH_3)_y^{(2-x)+}$. The ammine ligands have been shown to afford volatilization at low temperatures, and the hydroxo Zn complexes readily undergo a condensation reaction via olation or oxolation accompanying subsequent elimination of water at low temperatures. The simplified overall reaction can be expressed by the following reaction:

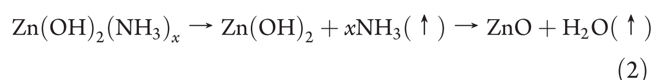

$$Zn(OH)_2(NH_3)_x \rightarrow Zn(OH)_2 + xNH_3(\uparrow) \rightarrow ZnO + H_2O(\uparrow) \quad (2)$$

The solution-processed ZnO-TFTs were evaluated to understand the influence of the pH. Figures 3 and 4 show the resulting electrical characteristics for transistors prepared from both the acidic and basic aqueous Zn solutions, respectively. Table 1 summarizes the important TFT characteristics such as field-effect mobility, threshold voltage, and on/off current ratio. The transfer curves indicate the operation of *n*-channel, enhancement-mode TFTs, as expected. In the case of acidic conditions, TFTs are inactive under 350 °C (Figure 3). Below this temperature, both solvent and organic species exist as obstacles in the films, hindering the formation of metal oxide films, as confirmed by the XRD results, which are discussed later. ZnO-based TFTs become operable when the semiconductor film is annealed at 400 °C (see Supporting Information, Figure S2), although a low mobility, high threshold voltage and large hysteresis are

Table 1. Electrical Characteristics of ZnO-TFTs Fabricated on SiO_2/n^+-Si Substrates in Acidic and Basic Aqueous Zn Solutions[a]

pH condition	samples	annealing temperature (°C)	mobility ($cm^2\ V^{-1}\ s^{-1}$)	threshold voltage (V)	on/off current ratio
acid	acid 150	150			
	acid 250	250			
	acid 350	350			
	acid 450	450	0.19	12.9	10^5
base	base 150	150	0.42	11.8	10^6
	base 250	250	2.95	2.2	10^7
	base 350	350	7.65	0.7	10^7
	base 450	450	14.70	−7.1	10^6

[a] Annealing was performed for 2 h in the temperature range of 150−450°C.

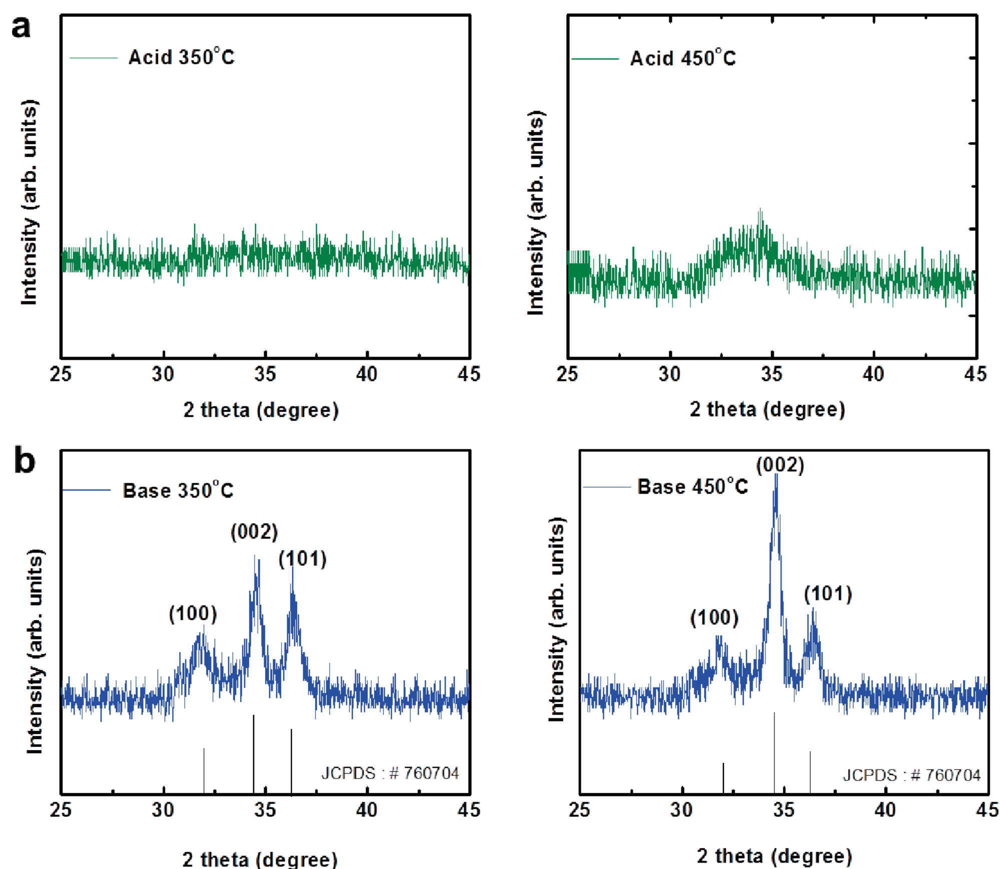

Figure 5. (a, b) XRD patterns of the aqueous Zn precursor-derived layers annealed at different temperatures and pH values of the aqueous precursors.

observed. The lower device performance may be due to remaining organic residue, as confirmed by the FT-IR analysis. The ZnO-TFTs produced under acidic conditions performed reasonably when the semiconductor film was annealed at 500 °C (see Supporting Information, Figure S3), where the performance is comparable to the film prepared from the basic aqueous solution and annealed at 250 °C.

The characteristics of the TFTs fabricated from the basic solution exhibit improved device performance with increased mobility and a higher on-current value compared to those produced from the acidic solution at the same temperatures (Figure 4). The TFTs operate well when the semiconductor films were annealed at 150 °C, and they still show hysteresis. When annealed at temperatures over 250 °C, the transfer curves obtained by positive- and negative-bias sweeps are nearly identical, indicating a lack of hysteresis. When annealing at temperatures below 250 °C, the semiconductor layer contains some polar groups such as ammine groups, which can induce hysteresis. When increasing the annealing temperature from 150 to 450 °C, the on current increased and the saturation mobility also increased from 0.42 to 14.7 $cm^2\ V^{-1}\ s^{-1}$. In addition, the threshold voltage shifted toward the negative voltage direction. We also fabricated the ZnO-TFTs using the precursor solution prepared by dissolving $Zn(OH)_2$ in an organic base of tetramethyl ammonium hydroxide. The resulting ZnO-TFTs annealed at 250 °C still operated although the performance was not comparable to that of the ammonia-based ZnO-TFTs because of the organic residues (see Figure S4, Supporting Information). This supports that the preparation of TFT under basic conditions is a prerequisite for low temperature device performance since the as-coated films contains a hydroxyo ligand that easily transforms to ZnO, while other ligand types (i.e.,

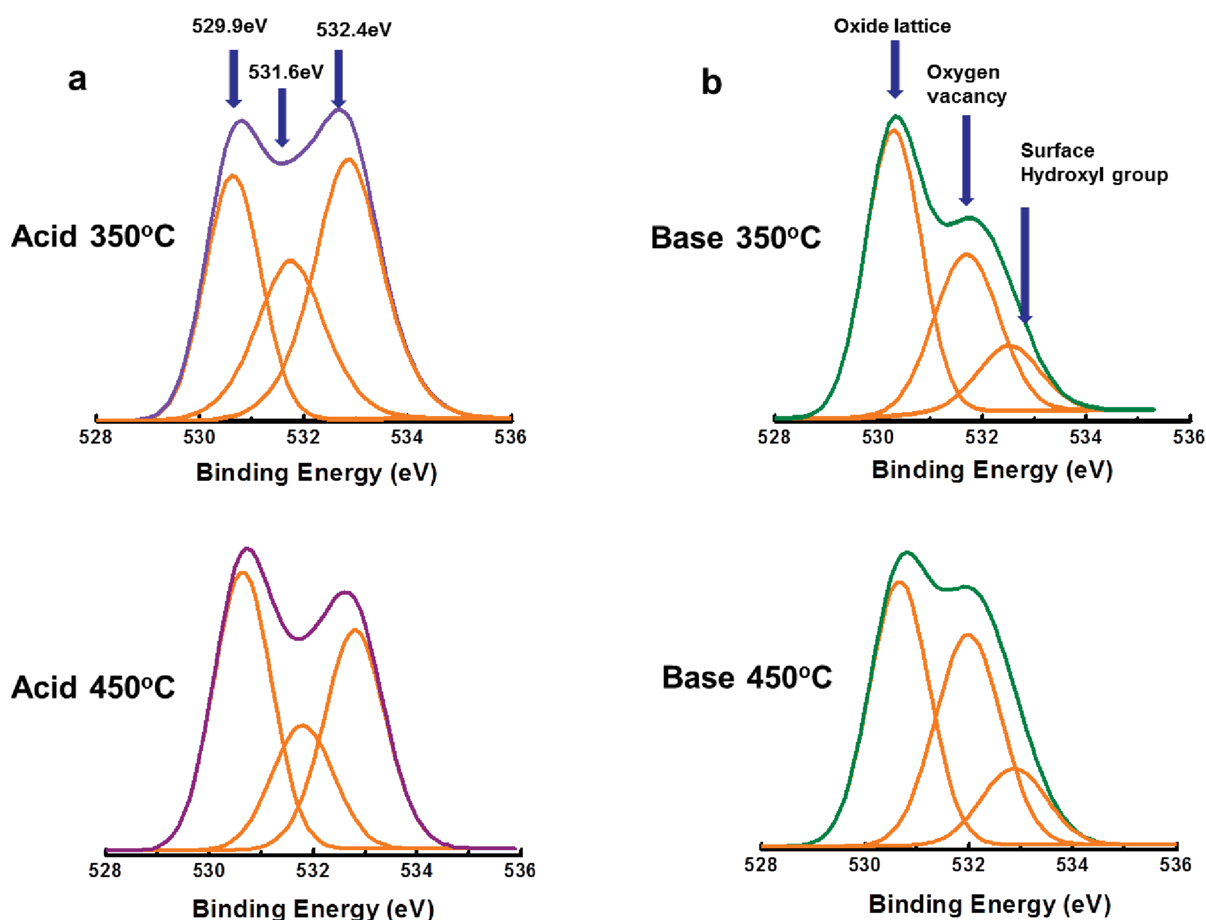

Figure 6. (a, b) XPS spectra of the aqueous Zn precursor-derived layers annealed at different temperatures and pH values of the aqueous precursors. The scan step size was 0.1 eV.

ammine and tetramethylammonium ion) influence the device characteristics.

The X-ray diffraction patterns shown in Figure 5 reveal the variations of the film crystallinity as a function of the annealing temperature and pH conditions of the aqueous precursors. The films obtained from the basic solution exhibit diffraction patterns consistent with the hexagonal wurtzite structure of ZnO. As manifested by the prominent (002) reflection observed at 34.3°, these films demonstrate a varying degree of *c* axis orientation, which increased significantly with elevated annealing temperature. Substantial *c*-axis orientation is frequently reported for high temperature deposited ZnO films from solution processes, as the grain growth tends to favor the low energy (002) surface.[22] In contratst, the film prepared from the acidic solution annealed at 350 °C exhibited amorphous-like broad peaks. The crystalline phase emerges for the sample annealed at 450 °C but showed no significant diffraction peaks. The XRD analysis clearly indicates that the films prepared from the acidic solution undergo slow crystallization to ZnO at 350 °C, hindered by the presence of anion/organic ligands, as confirmed by the FT-IR analysis. On the other hand, the film produced from the basic solution is well crystallized at the same annealing temperature of 350 °C. This means that the hydroxo−zinc complex can be converted to crystalline ZnO by dehydration at a low temperature, and the ammine ligand does not inhibit the crystallization of ZnO. Even the transitors annealed at 150 °C are active, indicating that the dehydration occurs below 150 °C, such that semiconducting characteristics can develop even if the ammine complex is still present. These results also explain the improved performance of the transistors prepared under basic conditions compared to those prepared under acidic conditions. An enhanced field effect mobility would result from better crystallization and preferred orientation of the grain structure, as indicated by larger grain sizes associated with ZnO films prepared from the basic solution relative to that produced under acid conditions (see Figure S5).

The chemical and structural evolution of the ZnO films as a function of the annealing temperature was analyzed by X-ray photoelectron spectroscopy (XPS). In principal, the properties of oxide semiconductor materials are strongly dependent on their bulk defect structures. Figure 6a and b show the O 1s XPS spectra of the aqueous Zn precursor-derived films as functions of the annealing temperature and pH. The XPS peaks for the O1s core level could be consistently fitted by three different near-Gaussian subpeaks, centered at 529.9, 531.6, and 532.4 eV. The dominant peak centered at 529.9 eV was assigned to the O^{2-} ion in a wurtzite structure surrounded by Zn atoms with their full complement of four nearest neighbor O^{2-} ions.[31] The peak at 531.6 eV was associated with the O^{2-} ion in oxygen-deficient regions. The binding energy peak at 532.4 eV was attributed to the presence of hydroxyl groups on the surfaces.[5] The peak area at 531.6 eV reflected oxygen vacancies as well as composition imperfections at the surface. Because hydrogen is more electronegative than metals, the oxygen atoms in the M−OH species are less negatively charged than those in the oxide, resulting in a shift

toward a higher binding energy. According to the XPS data, the films prepared from the acidic solution annealed at 350 °C are composed primarily of surface hydroxyl groups. Note that the film fabricated under acidic conditions annealed at 450 °C mainly consists of an oxide lattice with a small quantity of surface hydroxyl groups. The conduction band minimum in oxide semiconductors should be mainly composed of a dispersed vacant state with short intercation distances for efficient carrier transport,[1] which can be achieved in metal oxide lattices but not as easily in hydroxide lattices. Therefore, it is reasonable that metal-oxide-lattice formation is an essential prerequisite for ZnO films with good device properties. This is in accord with the aforementioned observations that ZnO-TFTs prepared from the acidic solution annealed below 350 °C are inactive, while those annealed at 450 °C are operable.

The semiconductor layer produced from the basic solution at 350 °C primarily consists of oxide lattices with minimal hydroxide content and a large amount of oxygen vacancies. In the solution-processed oxide films, it is generally accepted that oxygen vacancies in such systems are produced via polycondensation and dehydroxylation/dehydration processes during the annealing of the film. The surface hydroxyl groups (M−OH) are dehydroxylated and dehydrated upon heat treatment, releasing H_2O (from one hydroxyl + one hydrogen) and creating oxygen vacancies.[32] The XPS results imply that the channel layers fabricated under basic conditions result in better formation of the oxide lattice and oxygen vacancies, as compared to the samples produced from the acidic solution. Under basic conditions, the relative concentration of oxygen vacancies inside the ZnO films increases with the annealing temperature. The oxygen vacancy generation depends primarily on the annealing temperature. The formation of the oxygen vacancies involves electronic carrier generation in the oxide semiconductor.[33] As shown in Table 1, the on current and the saturation mobility increased as the annealing temperature was increased. These can be explained by the increased charge carriers upon the creation of more oxygen vacancies. However, the threshold voltage decreased with increasing annealing temperature. It is a consequence of the higher (absolute) number of free charges in the bulk, leading to easier accumulation of charges at the semiconductor/dielectric interface than the semiconductor with fewer charge carriers.[34] This results in the threshold voltage shifting toward the negative voltage direction. A decreased on/off current ratio with increasing annealing temperature is also related to the increased charge carriers upon the creation of more oxygen vacancies. Higher free charge carriers in the semiconductor lead to an increased off current, thereby reducing the on/off current ratio.

CONCLUSIONS

We investigated the influence of pH and ligand type on aqueous solution precursor-derived ZnO-TFTs. The pH is an important factor in determining the primary ligand type complexed with the metal cation in the aqueous solution. The soluble Zn complexes with a specific ligand in the solution have a predominant effect on the chemical characteristics of the aqueous solution-based ZnO semiconductors and, in turn, the resulting device performances of the TFTs. We characterized the electrical properties of the ZnO-TFTs deposited under both acidic and basic conditions in conjucntion with chemical and structural investigations using TG-DSC, FT-IR, XRD, and XPS. In contrast to the acidic aqueous solution, the use of basic aqueous Zn precursors leads to high performance oxide TFTs because the pathway involves a lower energy barrier for the solution-to-solid conversion. The film prepared under acidic conditions is mainly composed of hydrated zinc salt since the stable solution species of Zn is Zn^{2+} at low pH. It undergoes more complex reactions such as anion decomposition and dehydroxylation/dehydration, which require higher thermal energy to proceed. Ammine−hydroxo zinc complexes such as $Zn(OH)_x(NH_3)_y^{(2-x)+}$ are stable under basic conditions, which can easily transform to dense ZnO by dehydration and condensation at a lower temperature without significant organic residue. This difference leads to the enhanced device charateristics including a mobility of 0.42 $cm^2\ V^{-1}\ s^{-1}$ and an on/off current ratio of $\sim 10^6$ for the ZnO-TFTs annealed at 150 °C. In contast, the TFTs prepared under acidic conditions were inactive until the annealing temperature reached 400 °C. Our results suggest that solution-processable oxide semiconductors have the potential for low-temperature and high-performance applications in transparent, flexible devices.

METHODS

Preparation of ZnO Films. The 0.1 M Zn solutions for the ZnO layer were prepared by directly dissolving zinc hydroxide ($Zn(OH)_2$, 98%, Junsei, Japan) in an aqueous ammonia solution (NH_3, 25%, Alfa Aesar), resulting in a clear solution of pH 13.5. The 0.1 M Zn solutions were prepared by dissolving zinc hydroxide in an aqueous acetic acid solution (CH_3COOH, 99.7%, Sigma Aldrich), resulting in a solution pH of 4.7. The 0.1 M Zn solution was also produced by directly dissolving zinc hydroxide in an organic base solution of tetramethylammonium hydroxide ($(CH_3)_4N(OH)$, 23%, Sigma Aldrich), resulting in a transparent solution pH of ∼14. Prior to coating, the precursor solutions were rigorously stirred for ∼12 h at room temperature and filtered through 0.2 μm membrane filters. Subsequently, the solutions were spin-coated at 2000 rpm for 25 s onto SiO_2(thermally grown, thickness (t) = 100 nm)/n^+-Si substrates. The coated layers on the SiO_2/n^+-Si substrates were annealed at 150, 250, 350, and 450 °C for 2 h on a hot plate under an ambient atmosphere.

TFT Fabrication and Electrical Measurement. To fabricate the transistor with top-contact electrodes, a 50-nm-thick Al source and drain electrodes were deposited by a thermal evaporator (pressure $\sim 10^{-6}$ Torr) through a shadow mask. The channel was 3000-μm-wide and 100-μm-long. The I−V characteristics for all transistors were measured in the dark in ambient air using an Agilent 4155C semiconductor parameter analyzer to determine the electrical performance of the transistors. The threshold voltage (V_{th}) was determined from the drain current $(I_{DS})^{1/2}$ vs gate voltage (V_{GS}) plots. The saturation mobility (μ_{sat}) was calculated using the following formula:

$$I_{DS} = \left(\frac{\mu_{sat} C_i W}{2L}\right)(V_{GS} - V_{th})^2$$

where C_i, W, and L are the capacitance of the gate dielectrics per unit area, channel width, and channel length, respectively. The device parameters reported in this article are the average values based on at least five measurements from 10 freshly prepared transistors.

Chemical and Structural Analysis. A pH meter (IQ 150, IQ Scientific Ins.) was used to measure the solution pH. The thermal behavior of the as-dried powders at 120 °C was monitored under an ambient atmosphere using a thermal gravimetric and a differential scanning calorimeter (TGA-DSC, SDT Q 600, TA Ins.). The samples were dried at 120 °C, below which both the acid and the base solvents can be evaporated. X-ray photoelectron spectroscopy (XPS, ESCA Probe, ThermoVG) was used to identify the relative oxygen vacancies

and the surface hydroxyl group in the films. The chemical structures of the aqueous Zn precursor-derived films were measured using a FT-IR spectrometer (Spectrum 100, Perkin-Elmer) as functions of the annealing temperature and solution pH. The crystal structures of the films were also analyzed using X-ray diffractometry using Cu K_α radiation (DMAX-2500, Rigaku).

ASSOCIATED CONTENT

Supporting Information. The electrical characteristics of ZnO-TFTs measured at various conditions, FE-SEM images, and thermogravimetry−differential scanning calorimetry. This material is available free of charge via the Internet at http://pubs.acs.org.

AUTHOR INFORMATION

Corresponding Author
*E-mail: jmoon@yonsei.ac.kr.

ACKNOWLEDGMENT

This work was supported by the Midcareer Researcher Program through an NRF grant funded by the MEST (Nos. 2009-0086302). It was also partly supported by the Second Stage of the Brain Korea 21 Project.

REFERENCES

(1) Nomura, K.; Ohta, H.; Takagi, A.; Kamiya, T.; Hirano, M.; Hosono, H. *Nature* **2004**, *432*, 488.
(2) Kumoni, H.; Nomura, K.; Kamiya, T.; Hosono, H. *Thin Solid Films* **2008**, *516*, 1516.
(3) Fortunato, E.; Barquinha, P.; Pimentel, A.; Goncalves, A.; Martins, R. *Phys. Stat. Sol. (RRL)* **2007**, *1*, R34.
(4) Fortunato, E.; Barquinha, P.; Pimentel, A.; Goncalves, A.; Marques, A.; Pereira, L.; Martins, R. *Thin Solid Films.* **2005**, *487*, 205.
(5) Fortunato, E.; Pereira, L.; Barquinha, P.; Bothlho do Rego, A. M.; Goncalves, G.; Vila, A.; Morante, J. R.; Martins, R. *Appl. Phys. Lett.* **2008**, *92*, 222103.
(6) Hoffman, R. L. *J. Appl. Phys.* **2004**, *95*, 5813.
(7) Noh, Y. Y.; Zhao, N.; Caironi, M.; Sirringhaus, H. *Nat. Nanotechnol.* **2007**, *2*, 784.
(8) Kim, D.; Jeong, S.; Shin, H.; Xia, Y.; Moon, J. *Adv. Mater.* **2008**, *20*, 3084.
(9) Beng, S. O.; Chensha, L.; Yuning, L.; Yiliang, W.; Rafik, L. *J. Am. Chem. Soc.* **2007**, *129*, 2750.
(10) Jeong, S.; Jeong, Y.; Moon, J. *J. Phys. Chem. C* **2008**, *112*, 11082.
(11) Sun, B.; Peterson, R. L.; Sirringhaus, H.; Mori, K. *J. Phys. Chem. C* **2007**, *111*, 18833.
(12) Chensha, L.; Yuning, L.; Yiliang, W.; Beng, S. O.; Rafik, L. *J. Mater. Chem.* **2009**, *19*, 1626.
(13) Meyers, S, T.; Anderson, J, T.; Keszler, D, A. *J. Am. Chem. Soc.* **2008**, *130*, 17603.
(14) Meyers, S. T.; Anderson, J. T.; Hong, D.; Hung, C. M.; Wager, J. F.; Keszler, D. A. *Chem. Mater.* **2007**, *19*, 4023.
(15) Fleischhaker, F.; Wloka, V.; Hennig, I. *J. Mater. Chem.* **2010**, *20*, 6622.
(16) Jun, T.; Song, K.; Jeong, Y.; Woo, K.; Kim, D.; Bae, C.; Moon, J. *J. Mater. Chem.* **2011**, *21*, 1102.
(17) Pierre, A. C. *Introduction to Sol-Gel Processing*; Kluwer Academic Publishers: Norwell, MA, 2002.
(18) Jolivet, J. P. *Metal Oxide Chemistry and Synthesis*; J. Wiley & Sons Inc: New York, 2003.
(19) Stumm, W.; Morgan, J. J. *Aquatic Chemistry*; Wiley-Interscience: New York, 1995.
(20) Reichle, R. A.; McCurdy, K. G.; Hepler, L. G. *Can. J. Chem.* **1975**, *53*, 3841.
(21) Yamabi, S.; Imai, H. *J. Mater. Chem.* **2002**, *12*, 3773.
(22) Brien, P. O.; Saeeda, T.; Knowles, J. *J. Mater. Chem.* **1996**, *6*, 1135.
(23) Kajikawa, Y. *J. Cryst. Growth* **2006**, *289*, 387.
(24) Koo, C.; Song, K.; Jun, T.; Kim, D.; Jeong, Y.; Kim, S.; Ha, J.; Moon, J. *J. Electrochem. Soc.* **2010**, *157*, J111.
(25) Shaporev, A.; Ivanov, V.; Baranchikov, A.; Polezhaeva, O.; Tret'yakov, Y. *Russ. J. Inorg. Chem.* **2007**, *52*, 1811.
(26) Sharma, R. K.; Rawat, D.; Pant, P. *J. Macromol. Sci., Part A* **2008**, *45*, 394.
(27) Bandyopadhyay, S.; Paul, G. K.; Roy, R.; Sen, S. K.; Sen, S. *Mater. Chem. Phys.* **2002**, *74*, 83.
(28) Xia, X.; Zhu, L.; Ye, Z.; Yuan, G.; Zhao, B.; Qian, Q. *J. Cryst. Growth* **2005**, *282*, 506.
(29) Tsai, M. T.; Chang, H. C.; Tsai, P. J. *Key. Eng. Mater.* **2008**, *368*, 326.
(30) Kisailus, D.; Schwenzer, B.; Gomm, J.; Weaver, J. C.; Morse, D. E. *J. Am. Chem. Soc.* **2006**, *128*, 10276.
(31) Fan, J. C. C.; Goodenough, J. B. *J. Appl. Phys.* **1977**, *48*, 3524.
(32) Bae, C.; Kim, D.; Moon, S.; Choi, T.; Kim, Y.; Kim, B.; Lee, J.; Shin, H.; Moon, J. *ACS Appl. Mater. Interface* **2010**, *2*, 626.
(33) Martins, R.; Barquinha, P.; Pereira, L.; Ferreira, I.; Fortunato, E. *Appl. Phys. A: Mater. Sci. Process.* **2007**, *A89*, 37.
(34) Barquinha, P.; Pimentel, A.; Marques, A.; Pereira, L.; Martins, R.; Fortunato, E. *J. Non-Cryst. Solids* **2006**, *352*, 1749.